Khan, F.U.; Guarnizo, G.; Martín-Mateos, P. Direct hyperspectral dual-comb gas imaging in the mid-infrared. In: *Optics letters, 45(19), Pp. 5335-5338 (2020)*

DOI: 10.1364/OL.402875

Direct hyperspectral dual-comb gas imaging in the mid-infrared

FARID ULLAH KHAN[1], GUILLERMO GUARNIZO[2] AND PEDRO MARTÍN-MATEOS[1,*]

[1]*Electronic Technology Department, Universidad Carlos III de Madrid, Leganés, Spain*
[2]*Physics Department, Universidad Carlos III de Madrid, Leganés, Spain*
**Corresponding author: pmmateos@ing.uc3m.es*

Received XX Month XXXX; revised XX Month, XXXX; accepted XX Month XXXX; posted XX Month XXXX (Doc. ID XXXXX); published XX Month XXXX

In this manuscript, we present and experimentally validate the first direct hyperspectral dual-comb gas imaging system operating in the mid-infrared region. This method provides an unmatched combination of super fine spectral characterization and high temporal resolution without the need for thermal contrast between the target molecules and the background. In a proof-of-concept experiment, the system has allowed us to perform precision hyperspectral imaging of butane in the 3.4 μm band with a time resolution of 1 second. © 2020 Optical Society of America

Direct dual-comb hyperspectral imaging in the near-infrared has very recently been demonstrated[1]. This novel precision spectro-imaging method is based on illuminating the experimental scenario with two closely matched optical frequency combs and detecting the diffusely reflected signal with a camera. In this arrangement, the dual-comb source is operated at inter-teeth offset frequencies that are below the Nyquist limit of the camera, hence enabling the direct reading of interferograms by the pixel array. The Fourier transformation of the signal detected by each pixel of the camera sensor yields the dual-comb spectrum. This method provides an accurate spectral and spatial characterization of the scene at regular video-rates thus permitting the study of dynamic samples. The technique features an ultra-high-optical resolution that is only restricted by the linewidth of the teeth of the combs and a spectral coverage that (even moderate) enables the analysis of the wide spectral resonances of complex molecules. These features make of this approach a tool that promises to revolutionize optical gas imaging. Nevertheless, the sensitivity of the systems presented to date [1–3] is strongly hindered by operating in the near-infrared. In this paper, the architecture of the first direct dual-comb hyperspectral gas imager operating in the mid-infrared (mid-IR) is presented and experimentally demonstrated.

Currently, regular optical gas imaging cameras are basically implemented using an infrared camera and a cooled narrow optical band pass filter mounted in front of the detector [4,5]. The range of wavelengths that the filter let through coincides with the main molecular transitions of the particular gas compounds of interest. Therefore, the camera readings are sensitive to absorption (or emission) by the target gas of background radiation that would otherwise reach the camera sensor. This is a widely employed approach which is almost routinely used in the industry nowadays to monitor gas leaks in hard to reach areas and harsh environments. Nonetheless, accurate gas identification is unfeasible, as any molecular lines absorbing within the range of the optical filter will be detected in an indistinguishable way. Furthermore the sensitivity is heavily marked by the existing thermal contrast. The results presented in this manuscript demonstrate that many of the performance aspects of current passive optical gas imagers can be strikingly improved by using dual-comb gas imaging.

Direct hyperspectral dual-comb imaging is enabled by a dual-comb source capable of generating ultra-low rate interferograms [1]. The ultra-high coherence between combs required for generating such signals has led to the use of electro-optic dual-comb sources [6–9]. Indeed, these dual-comb generators feature beat-note signals with linewidths that can reach mHz levels in the RF domain, thus enabling the generation of very long interferograms (low-sub-second rates are feasible) [10,11]. This enables the multiheterodyne detection of the dual-comb signal by each pixel of a video camera, with a suited spectral coverage, operating at regular video rates. In this manner, this approach permits the rapid simultaneous spatial and spectral characterization of the target sample to enable precision spectro-imaging with excellent temporal resolution.

In order to address the main technological challenges for generating highly coherent combs in the mid-IR, the architecture presented in this manuscript employs a near-infrared electro-optic dual-comb that is shifted to the mid-IR through difference frequency generation (DFG) [12–14]. In an all-fiber arrangement, a 1064 nm pump laser is combined with the near-infrared dual-comb to generate a DFG output in the 3.4 μm range. One of the main strengths of this particular approach, obviously besides the inherently high coherence between combs, is the outstanding flexibility for adjusting the spectral span and the teeth spacing (repetition rate). This allows for the generation of tailored dual-combs for specific applications thus optimizing SNR and acquisition times.

The architecture of the proposed system is presented in Fig. 1. The setup is basically comprised of two subsystems: an all-fiber mid-IR dual-comb generator and the free space illumination and detection

arrangement. Focusing first on the mid-IR dual-comb generator, a 1550nm continuous wave (CW) laser (EP1550-0-NLW, Eblana Photonics) is driven at 120 mA and 32.8°C by a low noise current and thermal control unit (LDC/E-Currentx00, Luz WaveLabs). An erbium doped fiber amplifier (EDFA) amplifies the incoming optical signal to approximately 20 dBm which is then divided into two optical paths using a 50:50 coupler. In both branches, the frequency of the signal is shifted by 40 MHz acousto-optic modulators (AOM, Gooch and Housego). During the experiments presented in this Letter, a slight frequency offset of 8 Hz is maintained between the two AOM frequencies (40 MHz and 40 MHz + 8 Hz). The driving signals of the AOMs are provided by a phase coherent multi-channel synthesizer (Holzworth Instrumentation). Two lithium niobate optical phase modulators (EOSPACE) are used in both paths to generate two optical frequency combs with marginally different repetition rates. To drive the phase modulators, two RF signals with frequencies f_{r1} = 18GHz and $f_{r2} = f_{r1}+1$Hz were employed, yielding a spectral compression ratio of 1.8×10^{10}. This configuration will enable the generation of two combs with an offset frequency of 8 Hz and a difference in repetition frequencies of 1 Hz, thus generating 1 s long interferograms. The level of RF power injected into the modulators permits to adjust the spectral coverage of the combs. The two resulting signals are then recombined using a second 50:50 coupler to give rise to the 1550 nm dual-comb seed. This near-infrared dual-comb is combined with the signal from a narrow linewidth (500 KHz) 1064 nm pump laser (DFB-1064-PM-200-CW, QPhotonics) with a maximum power of 200 mW on a wavelength-division-multiplexing fiber coupler and ~~focused~~ taken to a quasi-phase matched LN waveguide module (WD-3440-000-A-B-C, NTT Electronics). This module consists of ~~into~~ a periodically poled lithium niobate (PPLN) waveguide crystal, a thermoelectric cooler and a thermistor and provides an overall efficiency of 10 %. ~~(NTT)~~. The resulting mid-IR signal has a power of approximately 4 mW. Proper selection of the pump and the signal wavelengths have to be performed in conjunction with an accurate control of the temperature of the PPLN crystal in order to maximize the mixing efficiency.

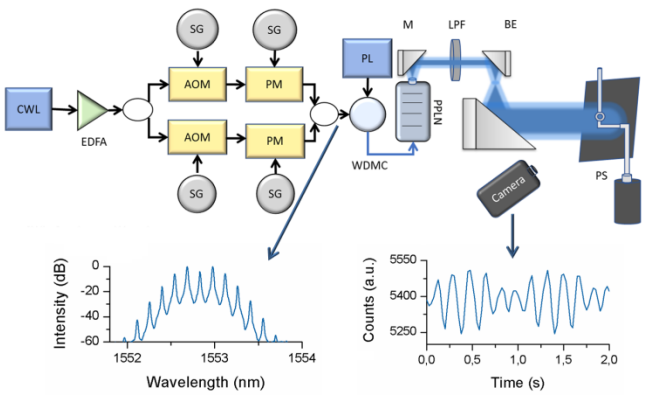

Fig. 1. Block diagram of the system. CWL, continuous wave laser; EDFA, erbium doped fiber amplifier; AOM, acousto-optic modulators; PM, phase modulator; SG, signal generator; PL, 1064 nm pump laser; WDMC, wavelength division multiplexing coupler; PPLN, periodically poled lithium niobate crystal; M, parabolic mirror; LPF, mid-IR filter; BE, beam expander; PS, piping system. The insets show (left) a typical spectrum of the near-IR dual-comb signal and (right) an actual example signal captured by a pixel of the camera.

The divergent mid-IR beam is first collimated by a parabolic mirror and then filtered to eliminate the residual near-infrared component. The diameter of the dual-comb beam is further expanded by an expander (comprised of two parabolic mirrors with different focal lengths) to increase the illuminated area on the target. The light reflected from the scene is collected by a cooled mid-IR camera (ORION SC7000, FLIR) with a 320x256 pixel sensor (for a spatial resolution of 0.5×0.5 mm) operating at 40 frames per second (the frame rate is synchronized with the rest of signals in the system). The raw video signal is post-processed (pixel by pixel Fourier transformation and normalization) to recover the final hypercube (spectral response measured by every single pixel of the camera).

To test the capabilities of the system, an experimental scenario consisting on a gas pipeline network (with a leaky joint) was implemented (shown in Fig. 2). This arrangement was placed at approximately 80 cm from dual-comb generator and the camera; the position of the camera was optimized to capture the highest intensity of signal reflected from the scene (this might be challenging in certain experimental scenarios for remote measurements in reflection configuration). The flow of butane was controlled by a manual valve. The experiments presented in the manuscript were performed using a dual-comb with nine teeth spaced by 18 GHz targeting butane gas at 3.37 μm (2967.7 cm^{-1}). As presented above the interferogram period is 1 s and the camera is operated at 40 frames per second.

Fig. 2. Photograph of the piping joint employed in the proof-of-concept experiment.

A first experimental demonstration can be seen in Figure 3, which shows the retrieved column density and the absorbance spectra at several spatial positions (the area illuminated by the dual-comb is identified by the blue color). This information is directly extracted from the ~~hypercube~~ spectrum retrieved for each pixel after intensity normalization to account for the different teeth amplitudes in the illumination signal. ~~using as a background~~As normalization reference an area of the image in which the gas is not present was used, even though ~~(~~ a measurement of the dual-comb using a reference detector could also be employed~~)~~. This step provides a characterization of the spectral transmittance measured by each pixel, from which column density and absorbance are straightforwardly obtained. For the calculation of the column density map a single interferogram is employed (40 frames) for a time resolution of a single second; no smoothening or noise reduction methods have been employed. These results demonstrate that direct dual-comb hyperspectral imaging in the mid-IR provides an utterly reconstruction of the concentration of gas in a scene. Indeed, this ability of the technique to precisely and rapidly characterize the optical spectrum of a two-dimensional scene with high optical and temporal resolution is in clear contrast with the limited performance of current methods. Figure 3 also shows the recovered average absorbance spectra at three spatial locations calculated for a matrix of 10 by 10 pixels (the integration time of these results is two seconds, 80 frames). The measured absorbance is fitted with a high resolution spectral characterization of butane, the residuals are also shown in the insets. The left topmost location shows an area in which no gas is present, as can also be seen from the column density map; a spectral absorbance of 0 (with a standard deviation of 0.005) is

obtained. By visualizing a second location (top right) in which the gas is present, the system provides an accurate measurement of the spectral absorbance. The best fit of the results demonstrates the ability of the architecture for yielding accurate spectral characterizations. At the bottom, an area with a higher gas concentration produces a stronger absorption that is precisely characterized by the method (as before, this is confirmed by the fit of the results).

As previously stated, direct dual-comb imaging provides not only tremendous spectral resolution but also a high temporal resolution due to the ability of these systems to operate with integration times equal to the interferogram period. To further illustrate this feature, Figure 4 shows four consecutive column density maps (extracted from four consecutive sets of forty frames each) that facilitate the monitoring of the dynamic behavior of gas leak. The temporal resolution is short enough so changes in the structure of the leak can be followed. This combination of super fine spectral characterization and high temporal resolution is indeed one of the main advantages of the approach demonstrated in this manuscript.

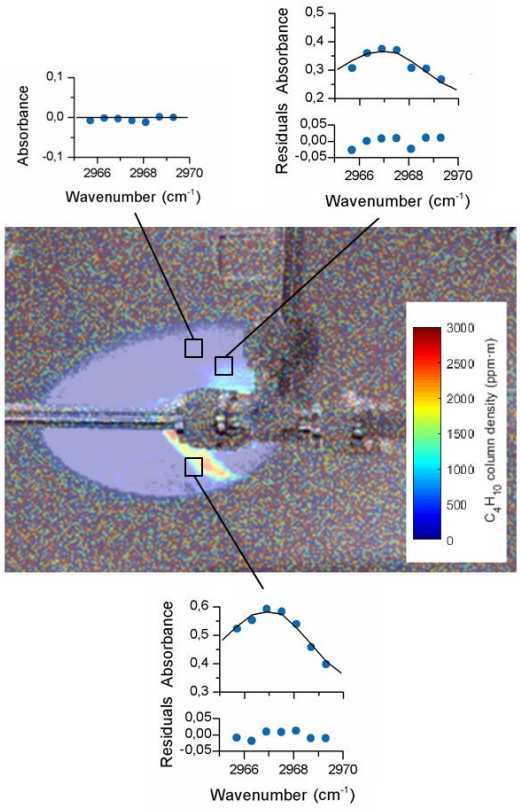

Fig. 3. Hyperspectral characterization provided by the direct dual-comb spectro-imager from a single interferogram merged with an original frame of the scene. The C_4H_{10} column density is retrieved from the measurement of absorbance at each pixel, the area illuminated by the dual-comb signal can be clearly identified. Three representative sample spectra (blue dot), obtained for a 10 by 10 pixel area and an integration time of 2 seconds are shown together with the fit of the results (black line).

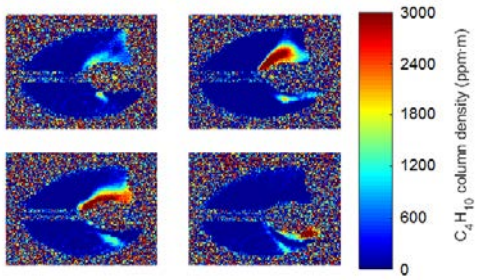

Fig. 4. Temporally resolved direct dual-comb hyperspectral images. Hyperspectral characterizations provided by the system at one second intervals (from left to right and top to bottom) showing the temporal evolution of the butane leak (results were calculated for an integration time of one second).

Precision dual-comb spectro-imaging of gas samples in the mid-IR has been demonstrated. This novel approach enables an unmatched (by any other hyperspectral or gas imaging method) and freely selectable optical resolution that is limited only by the linewidth of the teeth of the combs. The ability to perform super fine two-dimensional spectroscopy will allow forthcoming demonstrations not only to perform gas identification and measure gas concentration, but also to estimate the pressure and the temperature of the target compounds. Furthermore, this method can operate at very high temporal resolutions down to a single interferogram (only limited in practice by the camera frame rate and the number of teeth that are to be detected~~;~~). ~~i~~Indeed, the hyperspectral characterizations presented in this manuscript were performed simultaneously for all the pixels of the image in a single second. ~~For a given interferogram period, and a~~Δs with any other dual-comb system, the number of teeth that can be detected is restricted by the spectral resolution provided by the Fourier transformation after signal acquisition. In this particular demonstration a frame rate of 40 frames per second has enabled the precise measurement of the wide molecular transition of a complex molecule. Nevertheless, high-speed mid-IR cameras are becoming readily available, and this will enable to balance the performance of direct dual-comb spectro-imagers towards very high temporal resolution, towards having a large number of spectral points or as a trade-off between these two parameters. Due to the importance of this feature for gas imaging, it is noteworthy pointing out that the balance between integration time and number of teeth discussed above does not affect the spectral resolution of the system. Therefore, an arbitrarily fine optical resolution can be maintained with independence of a system configuration tilted to provide higher speeds or wider spectral coverages. This is clearly in contrast with modern infrared cameras equipped with Fourier spectrometers, which can only reach high spectral resolutions at the cost of several minutes of acquisition time[15].

In addition, regular gas imagers (based on both narrow band pass filters or Fourier spectrometers) require thermal contrast between the target gas and the background to operate properly. This feature provides one of the main strengths of these systems: the ability to operate remotely. Nonetheless, this same characteristic is responsible for instance for making gas clouds (with independence of the concentration) invisible as soon as diffusion processes equalize temperature with the surroundings and gas leaks undetectable unless there is a temperature difference. Direct dual-comb hyperspectral imaging, with an active interrogation approach, is not affected by the thermal contrast issue. This, consequently, together with the precision spectroscopy capabilities, offers the basis for revolutionizing the performance of optical gas imaging and for opening new application

opportunities. Future developments of the method will also provide higher optical intensity, a far larger illumination area and greater temporal resolution and spectral span; further widening the applicability of the technique.

Funding. This project has received funding from the ATTRACT project funded by the EC under Grant Agreement 777222 and from the Spanish Ministry of Economy and Competitiveness under Project TEC2017-86271-R.

Disclosures. The authors declare no conflicts of interest.

References

1. P. Martín-Mateos, F. U. Khan, and O. E. Bonilla-Manrique, Optica **7**, 199 (2020).
2. P. Martín-Mateos and G. Guarnizo, in Optical Sensors and Sensing Congress, p. FW5B.2 (2019).
3. T. Voumard, T. Wildi, V. Brasch, R. G. Álvarez, G. V. Ogando, and T. Herr, arXiv:2006.02115 (2020).
4. A. P. Ravikumar, J. Wang, and A. R. Brandt, Environ. Sci. Technol. **51**, 718 (2017).
5. Y. Zeng and J. Morris, J. Air Waste Manage. Assoc. **69**, 351 (2019).
6. D. A. Long, A. J. Fleisher, K. O. Douglass, S. E. Maxwell, K. Bielska, J. T. Hodges, and D. F. Plusquellic, Opt. Lett. **39**, 2688 (2014).
7. P. Martín-Mateos, B. Jerez, and P. Acedo, Opt. Express **23**, 21149 (2015).
8. G. Millot, S. Pitois, M. Yan, T. Hovannysyan, A. Bendahmane, T. W. Hänsch, and N. Picqué, Nat. Photonics **10**, 27 (2016).
9. V. Durán, S. Tainta, and V. Torres-Company, Opt. Express **23**, 30557 (2015).
10. A. J. Fleisher, D. A. Long, Z. D. Reed, J. T. Hodges, and D. F. Plusquellic, Opt. Express **24**, 10424 (2016).
11. P. Martín-Mateos, B. Jerez, P. Largo-Izquierdo, and P. Acedo, Opt. Express **26**, 9700 (2018).
12. E. Baumann, F. R. Giorgetta, W. C. Swann, A. M. Zolot, I. Coddington, and N. R. Newbury, Phys. Rev. A **84**, 062513 (2011).
13. M. Yan, P.-L. Luo, K. Iwakuni, G. Millot, T. W. Hänsch, and N. Picqué, Light Sci. Appl. **6**, e17076 (2017).
14. B. Jerez, P. Martín-Mateos, F. Walla, C. De Dios, and P. Acedo, ACS Photonics **5**, 2348 (2018).
15. M. Gålfalk, G. Olofsson, P. Crill, and D. Bastviken, Nat. Clim. Chang. **6**, 426 (2016).

References

1. P. Martín-Mateos, F. U. Khan, and O. E. Bonilla-Manrique, "Direct hyperspectral dual-comb imaging," Optica **7**(3), 199 (2020).
2. P. Martín-Mateos and G. Guarnizo, "Towards Hyperspectral Dual-Comb Imaging," in *Optical Sensors and Sensing Congress (ES, FTS, HISE, Sensors) (2019), Paper FW5B.2* (The Optical Society, 2019), p. FW5B.2.
3. T. Voumard, T. Wildi, V. Brasch, R. G. Álvarez, G. V. Ogando, and T. Herr, "Dual-Comb Real-Time Molecular Fingerprint Imaging," arXiv:2006.02115 (2020).
4. A. P. Ravikumar, J. Wang, and A. R. Brandt, "Are Optical Gas Imaging Technologies Effective for Methane Leak Detection?," Environ. Sci. Technol. **51**(1), 718–724 (2017).
5. Y. Zeng and J. Morris, "Detection limits of optical gas imagers as a function of temperature differential and distance," J. Air Waste Manage. Assoc. **69**(3), 351–361 (2019).
6. D. A. Long, A. J. Fleisher, K. O. Douglass, S. E. Maxwell, K. Bielska, J. T. Hodges, and D. F. Plusquellic, "Multiheterodyne spectroscopy with optical frequency combs generated from a continuous-wave laser.," Opt. Lett. **39**(9), 2688–2690 (2014).
7. P. Martín-Mateos, B. Jerez, and P. Acedo, "Dual electro-optic optical frequency combs for multiheterodyne molecular dispersion spectroscopy," Opt. Express **23**(16), 21149–21158 (2015).
8. G. Millot, S. Pitois, M. Yan, T. Hovannysyan, A. Bendahmane, T. W. Hänsch, and N. Picqué, "Frequency-agile dual-comb spectroscopy," Nat. Photonics **10**, 27–30 (2016).
9. V. Durán, S. Tainta, and V. Torres-Company, "Ultrafast electrooptic dual-comb interferometry," Opt. Express **23**(23), 30557–30569 (2015).
10. A. J. Fleisher, D. A. Long, Z. D. Reed, J. T. Hodges, and D. F. Plusquellic, "Coherent cavity-enhanced dual-comb spectroscopy," Opt. Express **24**(10), 10424–10434 (2016).
11. P. Martín-Mateos, B. Jerez, P. Largo-Izquierdo, and P. Acedo, "Frequency accurate coherent electro-optic dual-comb spectroscopy in real-time," Opt. Express **26**(8), 9700 (2018).
12. E. Baumann, F. R. Giorgetta, W. C. Swann, A. M. Zolot, I. Coddington, and N. R. Newbury, "Spectroscopy of the methane v3 band with an accurate midinfrared coherent dual-comb spectrometer," Phys. Rev. A **84**(6), 062513 (2011).
13. M. Yan, P.-L. Luo, K. Iwakuni, G. Millot, T. W. Hänsch, and N. Picqué, "Mid-infrared dual-comb spectroscopy with electro-optic modulators," Light Sci. Appl. **6**(10), e17076–e17076 (2017).
14. B. Jerez, P. Martín-Mateos, F. Walla, C. De Dios, and P. Acedo, "Flexible Electro-Optic, Single-Crystal Difference Frequency Generation Architecture for Ultrafast Mid-Infrared Dual-Comb Spectroscopy," ACS Photonics **5**(6), 2348–2353 (2018).
15. M. Gålfalk, G. Olofsson, P. Crill, and D. Bastviken, "Making methane visible," Nat. Clim. Chang. **6**(4), 426–430 (2016).